Journal of Applied Polymer Science

Oil sorption behaviors of porous polydimethylsiloxane modified collagen fiber matrix

Weining Du,[1,2] Xiaona Han,[1,2] Zhengjun Li,[1,2] Yupeng Li,[1,2] Lixin Li,[3] Kunyu Wang[1,2]

[1]National Engineering Laboratory for Clean Technology of Leather Manufacture, Sichuan University, Chengdu 610065, China
[2]Key Laboratory of Leather Chemistry and Engineering of Ministry of Education, Sichuan University, Chengdu 610065, China
[3]College of Chemistry, Sichuan University, Chengdu 610065, China
Correspondence to: Z. J. Li (E-mail: lizhengjun@scu.edu.cn)

ABSTRACT: A facial and cost-effective synthesis method of converting the leather protein solid wastes into a value-added collagen matrix oil sorbent is successfully established for the first time. Hide powder fiber (HPF) was firstly prepared by using the pre-tanned fleshing wastes from the leather industry, and then cross-linked with epoxy-terminated polydimethylsiloxane (PDMS) to produce hydrophobic collagen fiber, which was verified by the FT-IR spectrum and contact angle analysis. Subsequently, a series of porous PDMS modified collagen-based sorbents with roughness surface was successfully fabricated by solvent- and freeze-drying methods respectively. The oil sorption capacity, sorption saturated time and retention capacity of the prepared sorbents was investigated. Combined with the SEM images, liquid displacement method and contact angle analysis, the results revealed that oil sorption capacities of the sorbent with lower pore size, higher porosity and rougher surface for silicone oil, motor oil and vegetable oil were approximate to 13.60, 12.50, and 11.92 g/g, respectively. Additionally, the sorption of oils is a quasi-instantaneous process and also showed excellent oil retention capacity. It exhibited acceptable oil sorption performances as compared to commercial biomass sorbents. These findings indicated its potential as an eco-friendly oil sorbent material. © 2015 Wiley Periodicals, Inc. J. Appl. Polym. Sci. **2015**, *132*, 42727.

KEYWORDS: adsorption; biomaterials; fibers; porous materials

Received 20 May 2015; accepted 14 July 2015
DOI: 10.1002/app.42727

INTRODUCTION

Recently, oil spill accidents have occurred frequently in production, exploration or transportation, which have seriously affected marine ecology and human living environments.[1,2] Various methods can be used to remove floating oil from the water, for example, in situ burning, mechanical collection, biodegradation, and sorption approaches.[3] To date, oil sorbent materials have become increasingly attractive for oil cleanup thanks to their effectiveness, convenience and economy.[4]

Oil sorbents are able to concentrate and transform the liquid oils to the semi-solid or solid phase, which can then be removed the spilled oil in a convenient manner.[5] Currently, synthetic polymeric sorbents such as polyurethane foams,[6] polydimethylsiloxane sponge,[7] and electro-spun fiber,[8] have been widely used to clean up leaked oil due to their excellent oil sorption properties. However, these sorbents are non-renewable and lacking in biodegradability may cause negative impacts on the environment and consequently restrict their widely application. By contrast, natural polymeric sorbents such as cotton fiber,[9] kapok fiber,[10,11] wool fiber,[12] and collagen fiber[13,14] have attracted much attention in recent years because of their low cost, renewability and biodegradability. However, there are few in-depth researches on the oil sorbent prepared by protein fiber, in particular collagen fiber, as compared with commercial plant fiber sorbents.

Collagen fiber, a renewable biomass resource mainly exists in the animal skin tissue. During the leather-making such as fleshing and trimming processes generate substantial quantities of pre-tanned hide wastes, including abundant collagen fiber.[15] However, most of these solid wastes are disposed of through landfill or incineration processes, not only pose hazardous problem to the environment but also limit the reutilization of bio-resources.[16] Therefore, transforming these wastes into value-added products is extremely necessary.

Collagen fiber matrix has abundant functional groups such as —NH_2, —COOH, and —OH, etc., which provide abundant reactive groups to turn the surface from hydrophilic into hydrophobic through modification. Additionally, collagen fiber has a unique triple-helical structure, suggests that this structure can be conducive to form a hierarchical micro-structure between the fibers.

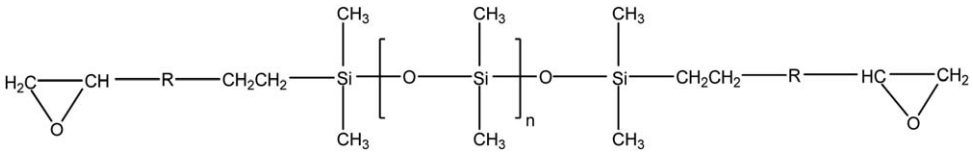

Scheme 1. The schematic molecular structure of ET-S.

To the best of our knowledge, few articles have reported the effect of the hydrophobicity and pore structures on the oil sorption performance of collagen fiber. In this study, hydrophobic collagen fiber was prepared by using an epoxy-terminated silicone oligomer (ET-S) as a modification agent. Recently, we have made a comparison study and demonstrated that ET-S oligomer cross-linked collagen fiber matrix exhibited high hydrophobicity-oleophilicity and good oil sorption capacities when compared with commercial tanned leather fibers. To make further research on the influence of the porous structure of PDMS modified collagen fiber matrix, different porosity and pore size of sorbents were fabricated via controlling the moisture content through solvent- and freeze-drying methods, which was inspired from previous literature.[17] Subsequently, oil sorption properties of as-prepared sorbents for silicone oil, motor oil, and vegetable oil in the pure oil and oil/water mixture systems were investigated. The findings demonstrate that by controlling pore characteristics and creating an even more hydrophobic surface, an eco-friendly sorbent can be prepared, suggest acceptable oil sorption properties similar to commercial plant fiber sorbents.

EXPERIMENTAL

Materials

Pre-tanned hide waste was obtained from a local tannery (Chengdu, China) in the splitting operation of bovine skin. Sodium carbonate, sodium bicarbonate, anhydrous ethanol, and acetone were purchased from Chengdu Kelong Chemical Co. The abovementioned reagents were analytically grade. ET-S ($M_n \approx 1000$) was supplied from the Tech Polymer Materials Co. (Shanghai, China). Its schematic molecular structure is shown in Scheme 1. Motor oil and vegetable oil were purchased from a supermarket (Chengdu, China). Silicone oil was kindly provided by China Bluestar Chengrand Research & Design Institute of Chemical Industry (Chengdu, China). The physical properties of these three kinds of oils are given in Table I.

Preparation of Hide Powder Fiber (HPF) and PDMS-Modified HPF

As described in previous literature,[18] procedures for preparing pre-tanned HPF were briefly as follows: edulcoration, demineralization, degreasing, dehydration, and milling. The de-limed fleshings were firstly cut into small pieces, and then washed with water to remove impurities. It was then soaked in an acetic acid-sodium acetate buffer (pH 4.6–5.0) for 1 d, and subsequently washed with water until neutral. This was followed by immersion in acetone overnight, and soaking in anhydrous ethanol. This procedure was repeated three times, until the color of the hide was nearly white. Finally, it was dried at room temperature, and then milled using a leather grinding machine (Dongyu machine factory, Zhejiang, China).

PDMS-modified HPF was prepared utilizing the above prepared raw HPF by a facile process. Typically, 2.715 g of ET-S was first dissolved in 21 mL of isopropyl alcohol in a flask. Then, 500 mL of Na_2CO_3-$NaHCO_3$ buffer solution and 30 g of raw HPF were added simultaneously, and the pH of the system was adjusted to 10.0. Subsequently, the system was reacted at 40°C for 24 h under a constant temperature shaking water bath (160 rpm). After that, the mixture was filtered and the separated fiber was washed with water and isopropanol to remove the unreacted reactants.

Preparation of Various Porous HPF Sorbents

The modified HPF was immersed in water and completely dispersed with a magnetic stirrer (HJ-6A, Jiangsu, China). Uniform sorbents (the moisture content is about 95%) were achieved using a paper shaper machine (ZT7-01, Shanxi, China). After that, the wet samples were pre-frozen at −18°C in a fridge for 24 h and dried. 95% (w/w) of freeze-dried sample (FD-95) was lyophilized (20 Pa, −50°C) in the vacuum freeze drier (FD-1A-50, Shanghai, China). 95% (w/w) of solvent-dried sample (AD-95) was placed in acetone until the film float on the liquid surface and dried at room temperature. 90% (w/w) of freeze-dried sample (FD-90) was obtained by firstly drying at room temperature for 24 h to decrease the water content, and then the wet sample was pre-frozen in a fridge, and finally lyophilized under the same condition.

Physicochemical Characterization Evaluations

FT-IR Spectra. The FT-IR analysis was performed on a Nicolet iS10 spectrometer (Thermo Fisher Scientific, USA) by using the KBr pellet method. Each spectrum was recorded at the resolution of 4 cm^{-1} in the spectral region of 4,000–400 cm^{-1}, with a total of 32 scans.

Contact Angle Analysis. Contact angle measurements were determined with an OCA20 contact angle system (Dataphysics, Germany) at 25°C. The drop size of the probe liquid was controlled to be 3.5 μL. The advancing/receding contact angle (θ_a/θ_r) were determined using the sessile drop method by increasing and removing 0.5 μL liquid from the existing droplet at a constant volumetric flow rate (0.15 μL/s), respectively.[19] Images of the droplets were recorded using an external video camera. The average contact angle values were obtained by conducting on five different positions. Young's equation was investigated to estimate the Young's contact angle (θ_Y) and coefficient of maximum static friction (λ).[20]

$$\lambda/\gamma_{gl} = (\cos\theta_r - \cos\theta_a)/2 \quad (1)$$

$$\cos\theta_Y = (\cos\theta_r + \cos\theta_a)/2 \quad (2)$$

wherein γ_{gl} ($mN \cdot m^{-1}$) is the surface tension of the probe liquid.

Table I. Physical Properties of Oils at Room Temperature (28 ± 2°C)

Oils	Density ($g \cdot cm^{-3}$)	Viscosity (mPa·s)	Surface tension ($mN \cdot m^{-1}$)	Weight loss after 24 h (%)
Silicone oil	0.96	90.5 ± 0.20	20.1 ± 0.06	0.0
Motor oil	0.88	153.0 ± 0.58	27.3 ± 0.35	0.0
Vegetable oil	0.91	48.5 ± 0.35	32.0 ± 0.17	0.0

± reference to standard deviation of the measured values.

Measurement of the Apparent Density

Apparent density (ρa) was tested by the ASTM D-285 methods,[21] which is defined as the weight of a material per unit volume it occupies in packing. Briefly, the length, width, and thickness of the sample were determined by using a vernier caliper. And then the weight of the sample was measured with an analytical balance. The apparent density was calculated by subsequent equation (3). Triplicate measurements were conducted and the average was obtained.

$$\rho_a = W_s / V_s \quad (3)$$

Measurement of the Porosity

Porosity was determined by the liquid displacement method. Typically, the pre-weighed sample (W_s) was placed into a graduated 25-mL bottle filled with anhydrous ethanol at 25°C. The total weight was recorded as W_1. After 24 h, liquids above calibration were imbibed, and the weight of the bottle was recorded as W_2. Then, the soaked sample was separated from the bottle, and the remainder was weighed as W_3. The porosity was calculated by the following eq. (4). Triplicate measurements were conducted and the average was obtained.

$$\text{Porosity} = (W_2 - W_3 - W_s)/(W_1 - W_3) \quad (4)$$

SEM Analysis

Longitudinal cross section images of as-prepared sorbents were obtained with a scanning electron microscope (Philips JSM-5900 SEM, Holland) at an acceleration voltage of 5 kV. The average pore size and its distribution were evaluated using Nano-measurer software (v1.2.5).

Determination of the Specific Surface Area

The specific surface area was measured by N_2-sorption by the BET model using an automatic surface area and porosimeter system (Micromeritics Tristar3000, U.S.A).

Evaluation of Oil Sorption Performance

Oil Sorption Capacity. In pure oil system: Approximately 0.2 g of the prepared sorbent (20 × 10 mm^2 surface area) was gently put into a 100-mL glass breaker containing 50 mL of oil for 10 min. After sorption, the sample was left to drip for 10 min and then weighted. Sorption capacity of the sorbents was calculated by the following equation (5).[8]

$$Q = (W_f - W_i)/W_i \quad (5)$$

where Q is the oil sorption capacity (g/g), W_i is the initial weight of the sorbent (g), and W_f is the final weight of the wet sorbent after draining or drying (g).

In oil/water system: 10 g of oil was mixed with 100 mL of distilled water in a 150-mL glass breaker, forming an oil layer approximately 3.0 mm thick on the surface of the water. Then, 0.2 g of sorbent was placed onto the surface of the oil for 10 min. Thereafter, the sorbent was transferred to a stainless-steel mesh, drained for 10 min, and placed on a glass petri dish and dried for 24 h at room temperature (28 ± 2°C). Finally, there was no significant change in weight of the sorbent sample, and the oil sorption capacity of the sorbents from water surface was determined according to the above eq. (5).[22]

Oil Sorption Saturated Time

For measuring oil sorption rate of the sorbents in pure oil medium, 0.2 g of sorbent was placed on the surface of oil in a glass breaker. Then, sorbent samples were isolated from oil at a specific times (0.5, 1, 2, 4, 6, 8, and 10 min) and drained for 10 min. The mass of absorbed oil was calculated by subtracting the initial sorbent weight from the total weight of the wet sorbent. Sorption capacity was computed using Equation (5), and the sorption saturation time was determined.

Oil Retention Capacity

The drainage process was also investigated to evaluate the retention capacity of as-prepared sorbents within a certain period. The test was performed according to the above-mentioned procedure of oil sorption. The weight of the sorbent was recorded after 0.5, 1, 2, 4, 6, 8, and 10 min drainage, and the retention of oil was determined by the following equation (6).[10,12]

$$Q_r = W_t / W_o \quad (6)$$

where Q_r is the retention of oil (%), W_t is the weight of the wet sorbent after t min dripping (g) (t = 0.5, 1, 2, 4, 6, 8, 10), and W_o is the weight of the sorbent before dripping (g).

RESULTS AND DISCUSSION

FT-IR Spectra

As shown in Figure 1, the peak at 3,424 cm^{-1} (stretching vibration peak of $-NH_2$) transfers to 3,398 cm^{-1}, implying that the decline of hydrogen bonds resulted from the crosslinking reaction. The band at 2,923 cm^{-1} (stretching vibration of C—H) in control fiber shifts to the position of 2,929 cm^{-1} in PDMS modified fiber, and the intensity of the peak slightly increases.[23] In addition, a group of new absorption peaks assigned to the symmetric stretching vibration of Si—O—Si appear at 1,058 cm^{-1}; 841 cm^{-1}; and 776 cm^{-1}.[23] These changes suggest that hydrophobic PDMS was cross-linked onto the surface of fiber.

Contact Angle

As shown in Table II, the Young's water contact angle (θ_Y) of all PDMS modified HPF samples was about 115°, shows higher

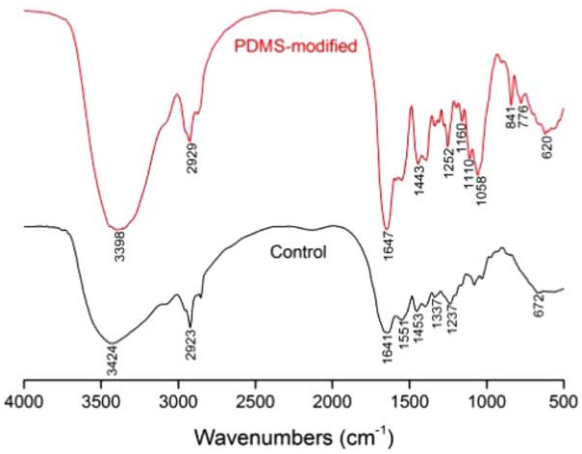

Figure 1. FT-IR spectra of control and PDMS-modified hide power fiber (HPF). [Color figure can be viewed in the online issue, which is available at wileyonlinelibrary.com.]

than that of the control HPF ($\theta_Y = 69.5 \pm 1.7°$), which is close to that of raw collagen fiber reported in the literature.[24] The above result indicates that the treatment significantly improves the hydrophobic property of pre-tanned fiber, being consistent with the FT-IR analysis results. Additionally, the coefficient of maximum static friction (λ) is proven increase as the contact angle (Δ between advancing and receding contact angle) increases. This renders the different rough surface, which can be ascribed to the different water content and dehydration method. Among them, the sorbent FD-95 exhibit a rougher surface, suggest a better sorption of oil.

Porosity, Specific Surface Area, and Pore Size

As shown in Table III, the apparent density of FD-95 was 0.058 ± 0.006 g/cm^3, that of AD-95 was 0.074 ± 0.018 g/cm^3, and that of FD-90 was 0.103 ± 0.008 g/cm^3. The corresponding parameters such as porosity and specific surface area increase with decrease of the apparent density. With higher water content sample and lyophilization dehydration method, the prepared sorbent FD-95 has a higher porosity and specific surface area as compared with the other two sorbents. It is favorable for the adhesion and adsorption of oil on its fiber surface and in its voids.

Figure 2 shows SEM images of the longitudinal cross section of prepared sorbents and their pore size distribution. As observed, there are certain amounts of continuous and interconnected pores among fibers, which are helpful for the absorption of oil onto the fiber surface. Furthermore, all these pores belong to macroprous structure. The pore size distribution was in the range of 10–200 μm for FD-95, 20–250 μm for AD-95, and 20–450 μm for FD-90. The average pore size of the sorbents was estimated to be 84.88, 129.24, and 155.35 μm for FD-95, AD-95, and FD-90, respectively (Table III).

Evaluation of Oil Sorption Properties

Oil Sorption Capacity. Figure 3(a) shows the oil sorption capacities of the FD-95, AD-95, and FD-90 sorbents for three typical oils in the pure oil system. Oil sorption capacity of FD-95 is higher than any other sorbents, and sorption capacity for silicone oil, motor oil, and vegetable oil is 13.60, 12.50, and 11.92 g/g, respectively. Table IV compares the oil sorption capacities of modified hide powder fiber sorbents (FD-95 HPF) to other biomass sorbents such as chrome shaving, wool fiber, silkworm cocoon waste, rice husk, milkweed fiber, kapok fiber, and modified kapok fiber for vegetable oil, motor oil, or engine oil, reported in the literatures. As can be clearly seen, the oil sorption capacities of HPF sorbents in this study is about two to seven times that of collagen matrix sorbents: chrome shavings,[13] and magnetic collagen fiber.[14] These results may be due to the hydrophobicity and roughness surface of the prepared sorbents. Additionally, this HPF sorbent also exhibits higher oil sorption capacities than that of plant sorbents such as rice husk[25] and milkweed fiber.[26] However, compared with the oil sorption capacities of wool fiber,[12] silkworm cocoon waste,[22] kapok fiber or modified kapok fiber[27] sorbents, the FD-95 HPF performance was inferior. Such behavior can be explained by the fact that the abovementioned researches was worked with loose fibers, that is, the oil sorption properties are closely related to the form of the fibers. As known from reported literature,[10] the FD-95 HPF shows a competitive oil sorption capacity as compared with raw kapok fiber sorbent at the same apparent density. The above results can be ascribed to the higher porosity and specific surface area of the FD-95, which provide a large amount of storage volume for absorbed oils. Meanwhile, the sorbent FD-95 exhibits lower average pore size and rougher surface, indicating that more oil can be trapped within its structure. The observed differences of oil sorption capacity were closely associated with the porosity, specific surface area, and pore size of sorbents.

As shown in Figure 3(a), sorption capacity of prepared sorbents for three oils increased in the following order: vegetable oil < motor oil < silicone oil. As known from previous report,[12] oil sorption capacity increases with the increasing of oil viscosity.

Table II. List of Advancing/Receding Contact Angle (θ_a/θ_r), Young's Contact Angle (θ_Y), and Coefficient of Maximum Static Friction (λ) of Prepared Sorbents

	Water contact angle (°)			
Samples	θ_a	θ_r	θ_Y	λ (mN/m)
Freeze-dry 95	130.3 ± 1.2	101.7 ± 1.82	115.3 ± 0.9	16 ± 1.14
Acetone-dry 95	126.5 ± 1.67	106.6 ± 0.65	116.1 ± 0.42	11.1 ± 1.23
Freeze-dry 90	118.1 ± 1.46	111.2 ± 1.28	114.6 ± 1.3	4 ± 0.43

Mean ± standard deviation, $n = 5$.

Table III. List of Apparent Density, Pore Size, Porosity, and Specific Surface Area of Prepared Sorbents

Samples	Apparent density (g/cm^3)	Specific surface area (m^2/g)	Porosity (%)	Average pore size (μm)
Freeze-dry 95	0.058 ± 0.006	0.8230	94.67 ± 0.33	84.88
Acetone-dry 95	0.074 ± 0.018	0.7558	93.39 ± 0.54	129.24
Freeze-dry 90	0.103 ± 0.008	0.5505	91.37 ± 0.47	155.35

Mean ± standard deviation, n = 3.

Surprisingly, obtained sorption capacities of silicone oil are higher than the higher viscosity motor oil. These results may be due to the lower surface tension of silicone oil, which can easily penetrate into sorbents and be retained in the voids. In addition, because of the chemical compatibility, the silicone oil can be firmly adhered on the surface of PDMS modified fibers. Therefore, viscosity and surface tension of oils were two vital parameters that influenced the sorption capacity.

In addition, sorption selectivity in oil/water mixtures is an important factor for oil sorbent in the practical oil spill cleanup. Figure 3(b) shows the oil sorption capacities of prepared HPF sorbents in the oil/water medium, lower than the corresponding data in the pure oil system. Among them, the FD-95 HPF also exhibits higher oil sorption capacity than the other two samples in the oil/water mixture system. The maximum oil sorption capacity of FD-95 HPF for silicone oil, motor oil, and vegetable oil is 12.02 g/g, 10.01 g/g, and 8.61 g/g, respectively. Moreover, the oil sorption decrease percentages of all the prepared samples for silicone oil are lower than the other two oils. This result can be attributed to the lower surface tension and higher viscosity of silicone oil, in particular the chemical component, which is similar to the discussions above.

Oil Sorption Saturated Time

Figure 4 exhibits the relationship between contact time and amount of oil absorbed per gram of sorbent. Obviously, oil sorption capacities of prepared sorbents almost reach the maximum within 1 min, and subsequently no significant change in oil sorption occurred when extending the contact time. That is, the sorption of oil is a quasi-instantaneous process, similar to the result obtained using chrome shavings to remove oil.[13] Such fast sorption rate is mainly due to the hydrophobicity rough surface and porous structures between the fibers, by which the oil can be easily penetrate into the fiber matrix.

As shown in Figure 4, sorption saturation time of prepared sorbents was in the order of silicone oil ≈ vegetable oil < motor oil, which is consistent with oil viscosity. This fact suggested that oil penetration into a capillary is inversely proportional to

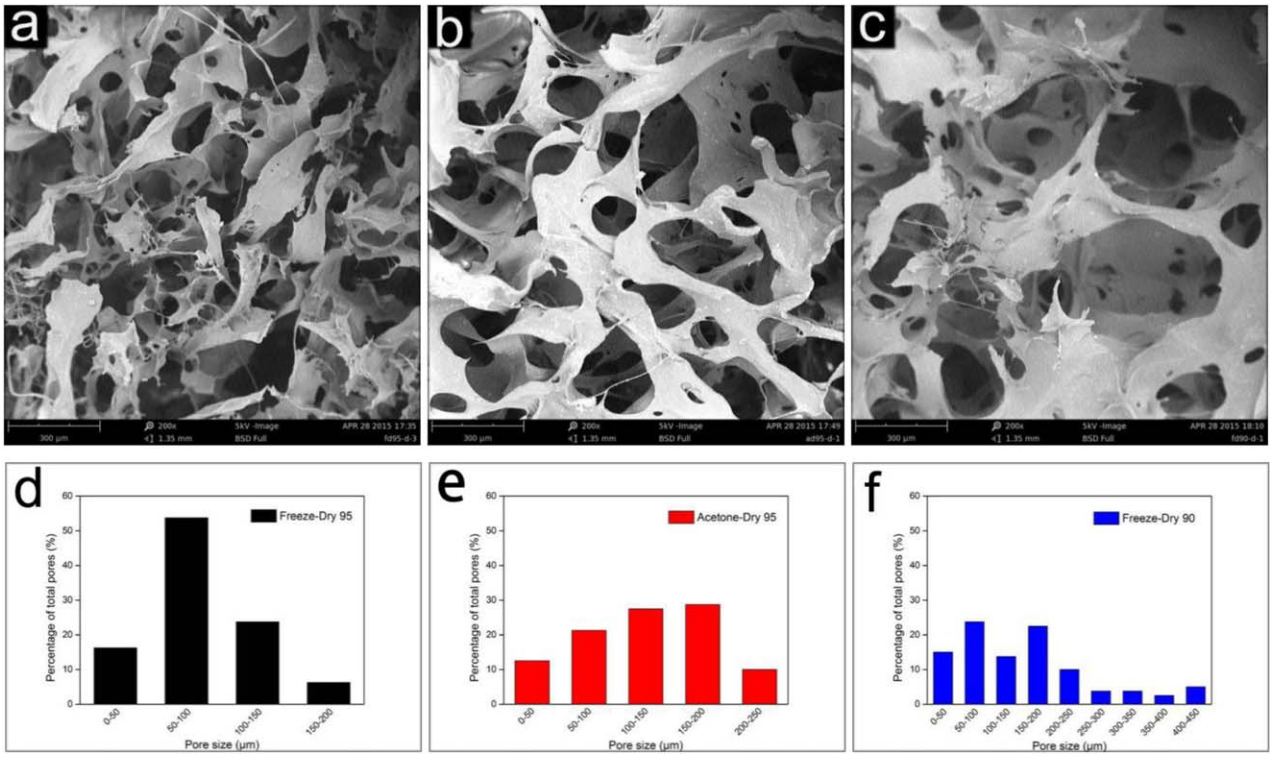

Figure 2. SEM images of longitudinal cross section (at a magnification of 200×) of (a) FD-95, (b) AD-95, and (c) FD-90. Pore size distribution of (d) FD-95, (e) AD-95, and (f) FD-90. [Color figure can be viewed in the online issue, which is available at wileyonlinelibrary.com.]

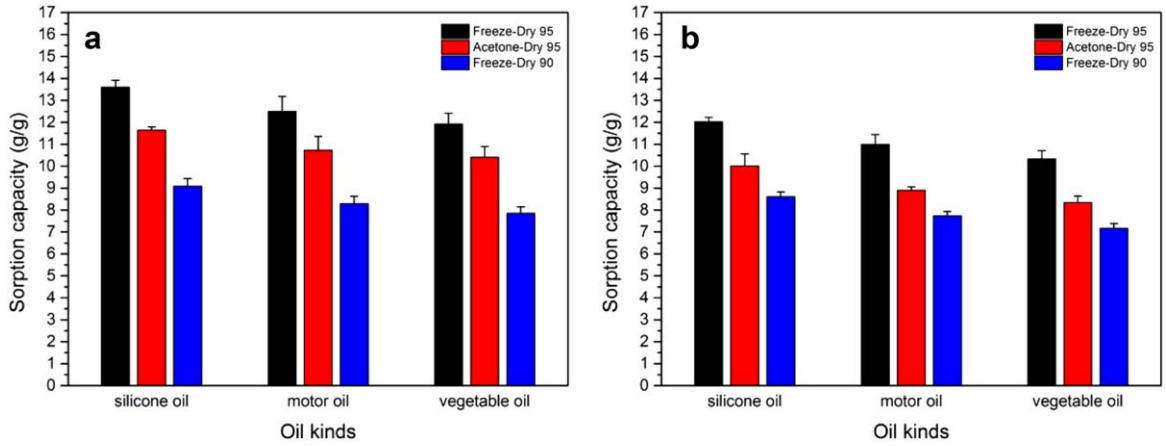

Figure 3. Maximum oil sorption capacity of prepared sorbents for three typical oils (a) in a pure oil system, and (b) in an oil/water mixture system. [Color figure can be viewed in the online issue, which is available at wileyonlinelibrary.com.]

Table IV. Comparison of Oil Sorption Capacities from This Study and Other Biomass Sorbents

Sorbent	Type of oil[a]	Oil sorption capacity (g/g)	Reference
Ground chrome shaving	Premium motor oil	7.6	[13]
Magnetic collagen fiber	Premium motor oil[b]	1.5	[14]
Recycled wool fiber	Motor oil	15.73	[12]
	Vegetable oil	14.48	
Silkworm cocoon waste	Motor oil	42–52	[22]
	Vegetable oil	37–60	
Rice husk	Engine oil	9.26	[25]
Milkweed fiber	Engine oil	10.8	[26]
Raw kapok fiber[c]	New engine oil	15.9	[10]
Raw kapok fiber	Soybean oil	49.1	[27]
Modified kapok fiber	Soybean oil	59.8	
FD-95 modified HPF	Silicone oil	13.60	This study
	Motor oil	12.50	This study
	Vegetable oil	11.92	This study

[a] Pure oil system.
[b] Oil mixed with water system.
[c] Packing density was 0.06 g/mL.

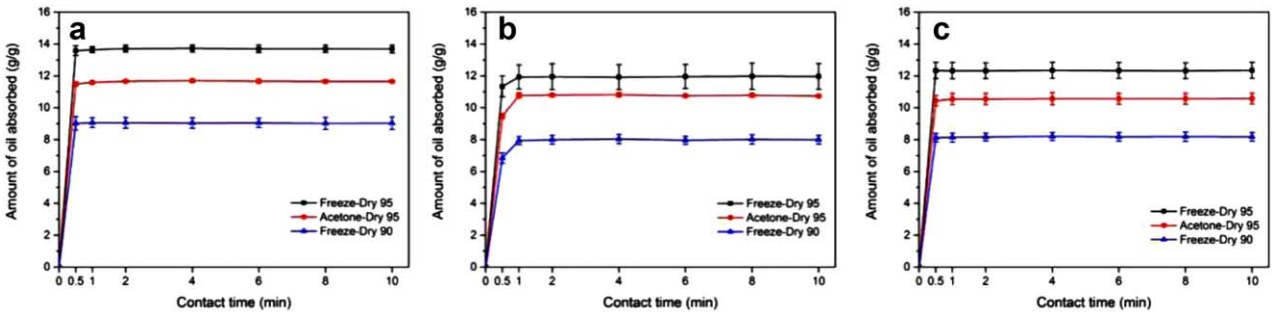

Figure 4. Amount of oil absorbed (g) per gram of sorbent versus contact time with three kinds of oils: (a) silicone oil, (b) motor oil, and (c) vegetable oil. [Color figure can be viewed in the online issue, which is available at wileyonlinelibrary.com.]

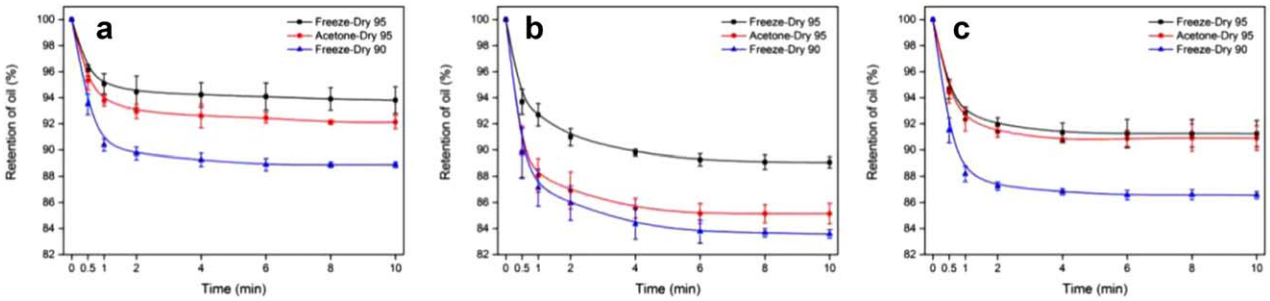

Figure 5. Oil retention capacity of prepared sorbents for three experimental oils: (a) silicone oil, (b) motor oil and (c) vegetable oil. [Color figure can be viewed in the online issue, which is available at wileyonlinelibrary.com.]

the oil viscosity.[11] However, the sorption saturation time has no difference between silicone oil and vegetable oil. This phenomenon may be due to the lower surface tension of silicone oil, which can be enhanced the wettability of the sorbent. Furthermore, the chemical component of PDMS modified fiber is similar to silicone oil, which contributes to the oleophilic interaction and van der Waals forces between the fiber surface and oil.

Oil Retention Capacity

Figure 5 shows retention percent of prepared sorbents for three types of oils. As observed, the sorbent FD-95 with higher porosity and specific surface area and lower pore size shows the highest retention percent among all sorbents, above 90% for three experimental oils. These facts indicate that the higher porosity and specific surface area of the sorbent, the larger interstice space for oil storage.[8] In addition, the sorbent with a lower pore size can inhibit the absorbed oil expelled from the pore structure. Furthermore, PDMS modified HPF sorbent exhibits excellent hydrophobicity–oleophilicity, which can contribute to the physical forces between fibers and oils, and enhance the oil retention capacity.

As shown in Figure 5, silicone oil displayed the highest retention capacity, above 90% for all prepared sorbents. This is probably due to its lower surface tension, and the stabilization of physical force between the fiber surface and oil, resulting in more oil molecules retained. However, retention capacity of the higher viscosity motor oil was less than that of the lower viscosity vegetable oil. It is well known that motor oil and vegetable oil have different components and polarities. Furthermore, PDMS modified HPF sorbent with a polar surface, is prone to absorb polar oils, so it is reasonable that the more polar vegetable oil would exhibit better retention capacity than motor oil.[28] Figure 5 also shows that oils with lower viscosity are prone to be released from sorbent at a faster rate and reach equilibrium sooner. For the high viscosity of motor oil, the sorbents can effectively retain the oil in the pores within the first two minutes of drainage, whereas the capillary pressure is insufficient to hold the weight of the oil for a longer time because of the gravity.[10]

CONCLUSION

In this study, a hydrophobic PDMS-modified HPF was prepared by silanization of raw HPF via a facile way. In addition, the effective porous structure of the sorbent played an even more important role in determining its oil sorption property. By controlling the water content and dehydration way, the sorbent with high porosity, large specific surface area, and low pore size could be achieved to obtain excellent oil sorption properties. These results suggest that wet sorbent with higher moisture content and dried by a lyophilization method can yield a suitable porous structure and favorable for oil sorption. Overall, we converted the sustainable pre-tanned leather protein wastes into an eco-friendly oil-sorbent material with acceptable oil sorption properties, which exhibits great potential for application in oil spill cleanup as compared to commercial plant fiber sorbent.

ACKNOWLEDGMENTS

The research was supported by the National Natural Science Foundation of China (No.21376153).

REFERENCES

1. Wang, J.; Zheng, Y.; Wang, A. *J. Appl. Polym. Sci.* **2013**, *127*, 2184.
2. Liu, H.; Liu, Z.; Yang, M.; He, Q. *J. Appl. Polym. Sci.* **2013**, *130*, 3530.
3. Feng, J.; Nguyen, S. T.; Fan, Z.; Duong, H. M. *Chem. Eng. J.* **2015**, *270*, 168.
4. Li, H.; Wu, W.; Bubakir, M. M.; Chen, H.; Zhong, X.; Liu, Z.; Ding, Y.; Yang, W. *J. Appl. Polym. Sci.* **2014**, 131. DOI: 10.1002/app.40080.
5. Karan, C. P.; Rengasamy, R. S.; Das, D. *Indian J. Fibre Text.* **2011**, *36*, 190.
6. Atta, A. M.; Brostow, W.; Datashvili, T.; El-Ghazawy, R. A.; Lobland, H. E. H.; Hasan, A. R. M.; Perez, J. M. *Polym. Int.* **2013**, *62*, 116.
7. Choi, S. J.; Kwon, T. H.; Im, H.; Moon, D. I.; Baek, D. J.; Seol, M. L.; Duarte, J. P.; Choi, Y. K. *ACS Appl. Mater. Interfaces* **2011**, *3*, 4552.
8. Wu, J.; Wang, N.; Wang, L.; Dong, H.; Zhao, Y.; Jiang, L. *ACS Appl. Mater. Interfaces* **2012**, *4*, 3207.
9. Singh, V.; Jinka, S.; Hake, K.; Parameswaran, S.; Kendall, R. J.; Ramkumar, S. *Ind. Eng. Chem. Res.* **2014**, *53*, 11954.
10. Abdullah, M. A.; Rahmah, A. U.; Man, Z. *J. Hazard. Mater.* **2010**, *177*, 683.

11. Wang, J.; Zheng, Y.; Kang, Y.; Wang, A. *Chem. Eng. J.* **2013**, *223*, 632.
12. Radetic, M.; Ilic, V.; Radojevic, D.; Miladinovic, R.; Jocic, D.; Jovancic, P. *Chemosphere* **2008**, *70*, 525.
13. Gammoun, A.; Tahiri, S.; Albizane, A.; Azzi, M.; Moros, J.; Garrigues, S.; Guardia, M. *J. Hazard. Mater.* **2007**, *145*, 148.
14. Thanikaivelan, P.; Narayanan, N. T.; Pradhan, B. K.; Ajayan, P. M. *Sci. Rep.* **2012**, *2*, 230.
15. Li, R.; Zhou, J.; Liao, X.; Zhang, W.; Shi, B. *J. Am. Leather. Chem. Assoc.* **2014**, *109*, 56.
16. Sundar, V. J.; Rao, J. R.; Muralidharan, C.; Mandal, A. B. *Crit. Rev. Environ. Sci. Technol.* **2011**, *41*, 2048.
17. Liu, C. K.; Latona, N. P.; Taylor, M. M.; Latona, R. J. *J. Am. Leather. Chem. Assoc.* **2012**, *107*, 70.
18. Brown, E. M.; Latona, R. J.; Taylor, M. M.; Garcia, R. A. *J. Am. Leather. Chem. Assoc.* **2012**, *107*, 1.
19. Woodward, R. P. Contact angle measurements using the drop shape method.; First Ten Angstroms Inc., Portsmouth, VA, **1999**.
20. Chen, X. Surface free energy and contact angle measurement of solid polymer; Central South University, **2012**.
21. ASTM 2007, D285. Refractories, Activated Carbon; Advanced Ceramics. West Conshohocken: PA, **2007**.
22. Moriwaki, H.; Kitajima, S.; Kurashima, M.; Hagiwara, A.; Haraguchi, K.; Shirai, K.; Kanekatsu, R.; Kiguchi, K. *J. Hazard. Mater.* **2009**, *165*, 266.
23. Reynolds, J. G.; Coronado, P. R.; Hrubesh, L. W. *J. Non-cryst. Solids.* **2001**, *292*, 127.
24. Ai, J.; Heidari, K. S.; Ghorbani, F.; Ejazi, F.; Biazar, E.; Asefnejad, A.; Pourshamsian, K.; Montazeri, M. *J. Nanomater.* **2011**, 1.
25. Ali, N.; El-Harbawi, M.; Jabal, A. A.; Yin, C. Y. *Environ. Technol.* **2012**, *33*, 481.
26. Rengasamy, R. S.; Das, D.; Karan, C. P. *J. Hazard. Mater.* **2011**, *186*, 526.
27. Wang, J.; Zheng, Y.; Wang, A. *Chem. Eng. J.* **2012**, *213*, 1.
28. Bacalum, E.; Cheregi, M.; David, V. *Rev. Roum. Chim.* **2012**, *57*, 427.